Polarization dependence of four-wave-mixing signals in quantum wells

D. Bennhardt and P. Thomas
Department of Physics and Materials Sciences Center, Philipps University, W-3550 Marburg, Federal Republic of Germany

R. Eccleston,* E. J. Mayer, and J. Kuhl
Max-Planck-Institut für Festkörperforschung, Heisenbergstrasse 1, W-7000 Stuttgart 80, Federal Republic of Germany
(Received 16 December 1992)

Recent transient four-wave-mixing experiments in the two-pulse photon-echo configuration performed on GaAs quantum wells have yielded the surprising result that in some samples the T_2 time obtained from the polarization decay can be shorter for cross-polarized input fields than for parallel input fields. A concomitant change from photon-echo to free-induction-decay behavior has also been observed. A phenomenological model is presented which explains these observations by means of a disorder-induced coupling of the σ^+ and σ^- exciton transitions which is inhomogeneous in coupling strength. Such coupling also leads to a remarkable change in the light-hole–heavy-hole exciton quantum beat phase as a function of pulse delay for a critical relative orientation of the polarization of the incident pulses. Experimental observations of this effect are presented to support the validity of the model.

INTRODUCTION

The polarization dependence of linear and nonlinear optical properties of semiconductors gives valuable information on their microscopic electronic structure. In particular, ultrafast optical spectroscopy studies of this polarization dependence have yielded a rich variety of data.[1–3] In the pioneering self-diffraction degenerate four-wave-mixing (DFWM) measurements of Abella, Kurnit, and Hartmann[1] on ruby the excited system was composed from two independent two-level absorbers with opposite circular polarization selection rules. In this particular situation the polarization of the DFWM signal is linear and rotated by an angle of $2\theta_{12}$ relative to that of the first pulse, where θ_{12} is the angle of the linear polarization vector of the second pulse with respect to that of the first pulse.

A similar system is realized by the heavy-hole exciton in GaAs/$Al_xGa_{1-x}As$ quantum wells. In this "circular model," there are also two independent oppositely circularly polarized (σ^+ and σ^-) transitions, since heavy-hole $m_j=\pm\frac{3}{2}$ states are connected to separate $m_j=\pm\frac{1}{2}$ electron states by optical dipole transitions [Fig. 1(a)].

However, in a number of recent self-diffraction DFWM experiments, it has been found that in some samples a different exciton dephasing rate is observed for the parallel ($\theta_{12}=0°$) and perpendicular ($\theta_{12}=90°$) polarization configurations.[2,3,6–8] This result is surprising since rotation of the polarization vectors of the incident fields merely alters the phase relationship between their constituent circular polarizations. There seems no reason why this phase shift should alter the dephasing efficiencies of the photocreated excitons. Up to now, no clear explanation for these observations exists.

It is the purpose of this paper to propose a phenomenological model which is able to account for this polarization-dependent dephasing time behavior. The

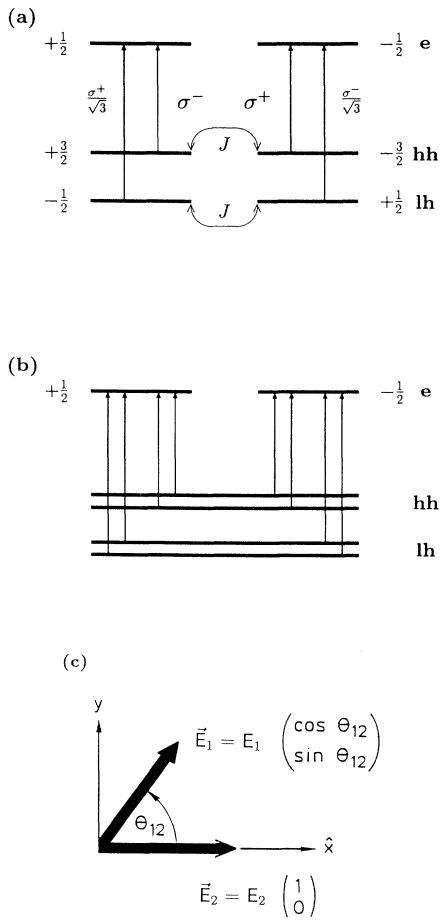

FIG. 1. (a) Level scheme and selection rules in a GaAs quantum well with coupling J. (b) Diagonalized level scheme. (c) Schematic diagram illustrating polarization notation employed in the text.

model generates the required change in dephasing time and also the apparent concomitant transition from photon-echo to free-polarization-decay behavior observed in time-resolved DFWM measurements.[3] The model also predicts a shift in light-hole–heavy-hole quantum beat phase as a function of delay at a critical angle. Experimental observations of this effect are presented to support the validity of our model system.

THEORETICAL

The central ingredient of our model is a coherent coupling of two of the degenerate levels in Fig. 1(a). In principle, there is no difference if the coupling is between the conduction-band or the valence-band levels. We consider here the second case, because the conduction-band states are pure spin states, while the valence-band states are partly mixed states, and the valence bands have a more complicated structure due to the quantum-well confinement potential. Possible microscopic mechanisms for the coupling can be the compositional disorder present in the $Al_xGa_{1-x}As$ barrier and the interface roughness as well as dislocations, stress effects, and impurities in the well.[4] This interaction with the disorder constitutes a local symmetry breaking, which has not been considered in the fundamental model of heavy-hole–light-hole quantum beats in Ref. 2. The excitonic heavy-hole and light-hole transitions are both twofold degenerate. The interaction with the disorder lifts the degeneracy in the hole levels,[4] thus coupling these levels with a certain coupling constant. The resulting eigenstates are sketched in Fig. 1(b). Up to now a quantitative microscopic calculation of the coupling is not yet obtained, but it will be the content of a later paper.

Note that in a single-particle picture this lifting of the degeneracy would not be possible, since the Kramers degeneracy requires at least twofold degeneracy. For the two-particle excitonic states discussed here the degeneracy is not necessary and the splitting of transitions is consistent with the time-reversal symmetry.

We calculate the signal in the photon-echo configurations using the optical Bloch equations for an $N\times M$-level system in the notation of Ref. 2:

$$\begin{aligned}
&\partial_t p_{mn}+i(\epsilon_n^c-\epsilon_m^v)p_{mn}+\gamma_{nm}^{cv}p_{mn} \\
&\qquad =i\sum_{m'} v_{mm'}R_{m'n}(t)-i\sum_{n'} R_{mn'}(t)c_{n'n}\ , \\
&\partial_t v_{mm'}+(i\epsilon_{m'}^v-i\epsilon_m^v+\gamma_{m'm}^{vv})(v_{mm'}-\delta_{mm'}) \\
&\qquad =i\sum_{n}[p_{mn}R_{m'n}^*(t)-R_{mn}(t)p_{m'n}^*]\ , \qquad (1) \\
&\partial_t c_{n'n}+i(\epsilon_n^c-\epsilon_{n'}^c)c_{n'n}+\gamma_{nn'}^{cc}c_{n'n} \\
&\qquad =-i\sum_{m}[R_{mn'}^*(t)p_{mn}-p_{mn'}^*R_{mn}(t)]\ .
\end{aligned}$$

To third order in the external light field and for δ-like laser pulses we get for the optical polarization in the kinematic direction $2\mathbf{k}_2-\mathbf{k}_1$,

$$\mathbf{P}^{(3)}_{2\mathbf{k}_2-\mathbf{k}_1}(t)=-i\Theta(t-\tau)\Theta(\tau)\sum_{n,m,n',m'}\mu_{nm}^* e^{-i(\epsilon_n^c-\epsilon_m^v-i\gamma_{nm}^{cv})(t-\tau)}(\boldsymbol{\mu}_{nm'}\cdot\mathbf{E}_{\mathbf{k}_2})(\boldsymbol{\mu}_{n'm}\cdot\mathbf{E}_{\mathbf{k}_2})e^{i(\epsilon_{n'}^c-\epsilon_{m'}^v-i\gamma_{n'm'}^{cv})\tau}(\boldsymbol{\mu}_{n'm'}\cdot\mathbf{E}_{\mathbf{k}_1})^*\ . \qquad (2)$$

Here pulse 1 acts first (at time 0) and generates a polarization which propagates for a time interval τ until pulse 2 arrives. The measured intensity is then given by (3) if all polarizations are detected, and by (4), if a polarizer is placed in front of the detector:

$$I_{\mathrm{FWM}}\propto\int dt\,|\mathbf{P}^{(3)}_{2\mathbf{k}_2-\mathbf{k}_1}(t)|^2\ , \qquad (3)$$

$$I_{\mathrm{FWM}}\propto\int dt\,|\,\mathbf{A}\cdot\mathbf{P}^{(3)}_{2\mathbf{k}_2-\mathbf{k}_1}(t)|^2\ . \qquad (4)$$

The vector $\mathbf{A}$ is a unit vector with the polarization direction of the polarizer. To describe different linear polarization orientations of the incident fields, we define an (x,y) coordinate system in the plane of the quantum well (QW) with $\mathbf{E}_2$ always lying along x and $\mathbf{E}_1$ at some angle θ_{12} to $\mathbf{E}_2$ [Fig. 1(c)]. On the basis of Fig. 1(a) we obtain the selection rules for the diagonalized 2×4 level scheme shown in Fig. 1(b) with the energy levels $(\varepsilon_{1/2}^c,\varepsilon_{-1/2}^c,\varepsilon_h^v+J,\varepsilon_h^v-J,\varepsilon_l^v+J,\varepsilon_l^v-J)$. Using the selection rules and eigenvalues of the coupled model we find from Eq. (2) the third-order nonlinear polarization

$$\begin{aligned}
\mathbf{P}^{(3)}_{2\mathbf{k}_2-\mathbf{k}_1}(t,\tau)=\frac{-i}{4}\Theta(t-\tau)\Theta(\tau)E_2^2E_1^*\Bigg[&\begin{bmatrix}\cos\theta_{12}\\0\end{bmatrix}\{|\mu_h|^2e^{-i(\varepsilon^c-\varepsilon_h^v-i\gamma_h^{cv})(t-\tau)}+|\mu_l|^2e^{-i(\varepsilon^c-\varepsilon_l^v-i\gamma_l^{cv})(t-\tau)}\} \\
&\times\{|\mu_h|^2e^{i(\varepsilon^c-\varepsilon_h^v+i\gamma_h^{cv})\tau}+|\mu_l|^2e^{i(\varepsilon^c-\varepsilon_l^v+i\gamma_l^{cv})\tau}\}\{e^{iJ(t-2\tau)}+e^{-iJ(t-2\tau)}\} \\
&+\begin{bmatrix}0\\-\sin\theta_{12}\end{bmatrix}\{|\mu_h|^2e^{-i(\varepsilon^c-\varepsilon_h^v-i\gamma_h^{cv})(t-\tau)}-|\mu_l|^2e^{-i(\varepsilon^c-\varepsilon_l^v-i\gamma_l^{cv})(t-\tau)}\} \\
&\times\{|\mu_h|^2e^{i(\varepsilon^c-\varepsilon_h^v+i\gamma_h^{cv})\tau}-|\mu_l|^2e^{i(\varepsilon^c-\varepsilon_l^v+i\gamma_l^{cv})\tau}\}\{e^{iJt}+e^{-iJt}\}\Bigg]\ . \qquad (5)
\end{aligned}$$

J is the coupling due to the disorder interaction. Since the coupling originates from disorder, we expect that there will not be a fixed value of J but rather a distribution of coupling strengths around an average value, which may be zero or finite. This distribution function certainly depends sensitively on the preparation conditions of a given sample, and may vary considerably from sample to sample. An upper bound for the width of the distribution function can be estimated from the linewidth of the excitonic transitions.

We assume a Gaussian distribution function $g(J)$ centered at an average value $J_0=0$, which produces a Gaussian envelope $g(t)=\int g(J)e^{iJt}dJ$ in the response signal. Note that it is the Fourier transform $g(t)$ of $g(J)$ that enters into our analysis:

$$\mathbf{P}^{(3)}_{2\mathbf{k}_2-\mathbf{k}_1}(t,\tau)=\frac{-i}{2}\Theta(t-\tau)\Theta(\tau)E_2^2E_1^*\left[\begin{pmatrix}\cos\theta_{12}\\0\end{pmatrix}\{|\mu_h|^2e^{-i(\varepsilon^c-\varepsilon_h^v-i\gamma_h^{cv})(t-\tau)}+|\mu_l|^2e^{-i(\varepsilon^c-\varepsilon_l^v-i\gamma_l^{cv})(t-\tau)}\}\right.$$
$$\times\{|\mu_h|^2e^{i(\varepsilon^c-\varepsilon_h^v+i\gamma_h^{cv})\tau}+|\mu_l|^2e^{i(\varepsilon^c-\varepsilon_l^v+i\gamma_l^{cv})\tau}\}g(t-2\tau)$$
$$+\begin{pmatrix}0\\-\sin\theta_{12}\end{pmatrix}\{|\mu_h|^2e^{-i(\varepsilon^c-\varepsilon_h^v-i\gamma_h^{cv})(t-\tau)}-|\mu_l|^2e^{-i(\varepsilon^c-\varepsilon_l^v-i\gamma_l^{cv})(t-\tau)}\}$$
$$\left.\times\{|\mu_h|^2e^{i(\varepsilon^c-\varepsilon_h^v+i\gamma_h^{cv})\tau}-|\mu_l|^2e^{i(\varepsilon^c-\varepsilon_l^v+i\gamma_l^{cv})\tau}\}g(t)\right]. \quad (6)$$

Consider first the parallel configuration, $\theta_{12}=0$. Here, the first term in the signal is dominant. It has an envelope centered at the time characteristic of a photon-echo signal, $t=2\tau$. Thus a photon echo is observed at 2τ for the parallel polarization configuration. The decay of this echo is determined by the (phenomenologically introduced) dephasing rates $\gamma_{h,l}^{cv}$. However, for the perpendicular configuration, $\theta_{12}=90°$, the first term is zero and the second term dominates. This has an envelope centered at time zero, which has to be multiplied by the causality function $\Theta(t-\tau)$. Thus no echolike signal is obtained but instead a signal, which has for $t>\tau$ the characteristic of a so-called free induction decay. For a slow (time-integrating) detector, the dephasing rate is then determined either by the phenomenological rates $\gamma_{h,l}^{cv}$ or by the width of the Fourier transform of the distribution function of J, depending on the relative magnitude of these quantities. The resulting apparent dephasing rate is therefore always equal or larger than that of the true dephasing rate observed in the parallel configuration. In Fig. 2 we have plotted time-integrated response signals for the following set of parameters: $\gamma_h^{cv}=(6\text{ ps})^{-1}$, $\gamma_l^{cv}=(4\text{ ps})^{-1}$, $\varepsilon_h^v-\varepsilon_l^v=6.28\text{ ps}^{-1}$ and width of the distribution function of J, $\Delta J=0.3\text{ ps}^{-1}$. It should be noted that these parameters are expected to be strongly sample dependent. Here, we have chosen a large but reasonable ΔJ value to emphasize the new physical effects. The signal has been calculated for $\theta_{12}=0°$, 45°, 60°, and 90° as a function of delay time. We have taken into account that heavy-hole (hh) transitions have smaller dephasing rates than light-hole (lh) transitions.[5] Figure 2 clearly shows the different apparent dephasing rates for parallel and perpendicular orientation.

As explained above, the transformation from photon-echo behavior to an apparent free-induction decay in time-resolved DFWM as a function of θ_{12} which accompanied the change in apparent dephasing rate reported in Ref. 3 is also explained by our model. Figure 3 shows explicitly the time-resolved self-diffraction signal, which is expected if only the heavy-hole exciton is excited.

The change in quantum beat phase between the parallel and cross-polarized beams has been explained previously.[2] In addition we show also the behavior at intermediate angles 45° and 60°. A remarkable change from the results expected from Ref. 2 is obtained. For the smaller angle 45°, the beats do not cancel but are in phase with those obtained for parallel orientation. Moreover, the relative beat amplitude increases with increasing delay time. This increase can be explained if one looks carefully at the two contributions in (6). The phases of the parallel (0°) and perpendicular (90°) contributions (first and second terms in square brackets) have a relative phase shift of π. For small delay times and $\theta_{12}=45°$ these in-phase and antiphase beating amplitudes tend to cancel: the beat amplitude is small. For larger delay times the perpendicular contribution decays faster than the parallel

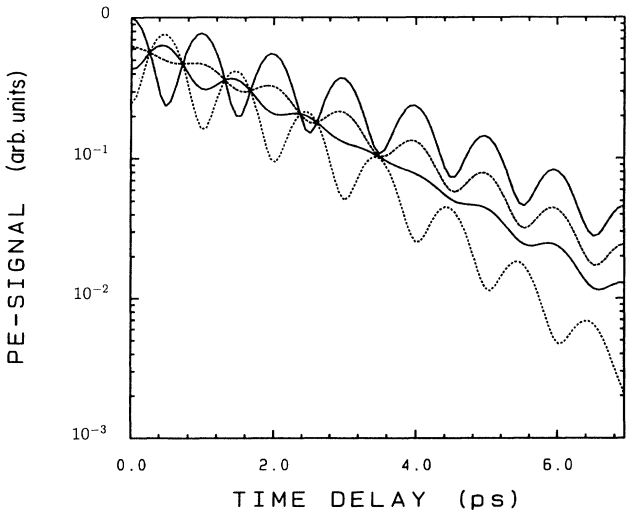

FIG. 2. Time-integrated signal in the photon-echo configuration for different orientations of the excitation pulses. From above: 0°, 45°, 60°, 90° (theoretical).

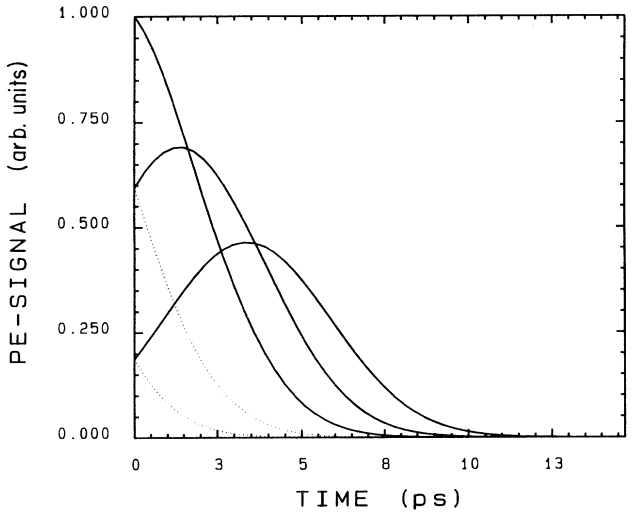

FIG. 3. Time-resolved signal in the photon-echo configuration for different delay times (0 ps, 2 ps, 4 ps) and polarization orientation (0°,90°) of the excitation pulses. Dashed lines, perpendicular orientation; solid lines, parallel orientation.

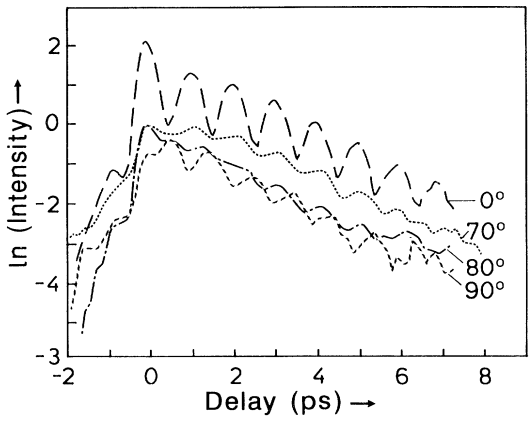

FIG. 4. Time-integrated signal in the photon-echo configuration for different orientations of the excitation pulses. From above: 0°,70°,80°,90° (experimental).

one due to the $g(t)$ envelope, so the in-phase beat amplitude increases. For larger angles a similar argument holds. However, at small delay the perpendicular antiphase beat contribution dominates. Thus a remarkable shift in the beat phase from antiphase to in-phase with increasing delay is predicted.

EXPERIMENT

We now give experimental evidence to support the validity of this inhomogeneous coupling of the σ^+ and σ^- transitions as an explanation of apparent θ_{12}-dependent dephasing times. As described above, we would expect (Fig. 2) a change in the lh-hh exciton quantum beat phase with pulse delay in samples where apparently different T_2 times are observed for the parallel and perpendicular polarization configuration. We performed experiments on a 20-nm single GaAs quantum well, with a 0.74-meV photoluminescence (PL) linewidth. The sample was maintained at 8 K in a continuous flow helium cryostat. The two-pulse self-diffraction measurements were performed in the reflection geometry at an excitation density of 1×10^9 excitons per cm^2. Tunable laser pulses of 1.3-ps duration and 16-cm^{-1} bandwidth were derived from a mode-locked Ti:sapphire laser. The signal was detected using a cooled GaAs photomultiplier tube. The polarization orientation of the input beams was adjusted using $\lambda/2$ plates, providing polarization definition of better than 100:1.

Figure 4 shows the time-integrated 2-pulse DFWM intensity in the $2\mathbf{k}_2-\mathbf{k}_1$ direction for different θ_{12} for no polarizer before the detector. The center of the laser spectrum was chosen to simultaneously excite roughly equal quantities of light- and heavy-hole excitons. The beat period was 1.1 ps, and was in good agreement with the lh-hh splitting determined from cw PL measurements.

We find that the dephasing time at $\theta_{12}=90°$ is only 70% of that measured at $\theta_{12}=0°$. Note first that the quantum beats at $\theta_{12}=90°$ are exactly 180° out of phase to those at $\theta_{12}=0°$. In a pure circular model, the crossover between in-phase and antiphase beating occurs at $\theta_{12}=45°$, where the beat amplitude should be zero. However, we find no such crossover. At $\theta_{12}=70°$ the beats remain in-phase with those at $\theta_{12}=0°$ and the relative beat amplitude increases with increasing delay time. At $\theta_{12}=80°$ we observe the appearance of antiphase beats at small delay, followed by a region where the beat amplitude becomes very small, and finally the reappearance of in-phase beating at longer delay. This behavior cannot be explained with the uncoupled circular model, but it is in good agreement with the prediction of the inhomogeneous coupling model, as described above.

It should be mentioned, however, that this theoretical model fails to explain the change of signal intensity with polarization configuration. In the experiments, the intensity for parallel polarization is four times higher than for perpendicular polarization of the two incident pulses, whereas the theory predicts the intensities to be the same.

In the context of the present work it is important that the prediction of the theoretical model for the critical angle (i.e., the angle for the change from antiphase to in-phase beating) is influenced by the relative intensity of parallel and perpendicular signal. In our case the intensity enhancement of the parallel in comparison to the perpendicular signal obviously leads to a shift of the critical angle to larger values as compared to the angle calculated in the theoretical model ($\theta_{12}=60°$). Exactly this result is shown in Fig. 4. We therefore conclude that our experiments support the validity of this model.

Finally we have investigated the ratio of T_2 measured for perpendicular ($T_2^{\perp}$) and parallel ($T_2^{\parallel}$) configuration in a wide variety of single quantum wells, and attempted to correlate this ratio ($R=T_2^{\perp}/T_2^{\parallel}$) with sample quality. The unavailability of a single quantity which directly measures sample quality of course makes such an investigation problematic, and the results can only be stated

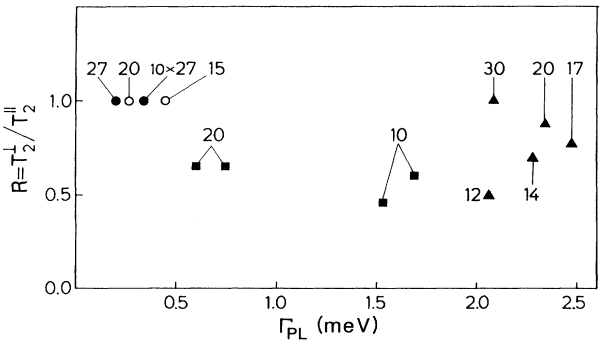

FIG. 5. Ratio of the experimental T_2 times measured for parallel and perpendicular polarization of the incident pulses vs photoluminescence linewidth for a variety of single QW samples and one multiple QW (black dot 10×27) grown in the laboratories of K. Ploog, MPI für Festkörperforschung, Stuttgart (black dots); R. Hey, Paul Drude Institut, Berlin (open circles); K. Köhler, Fraunhofer Institut für Angewandte Festkörperphysik, Freiburg (squares); and Y. Horikoshi, NTT Basic Research Laboratories, Musashino-shi/Japan (triangles). The numbers give the quantum-well thickness in nm.

tentatively. We take the photoluminescence linewidth as an approximate measure of the disorderliness of the samples. Our findings are summarized in Fig. 5. We find that the samples with a PL linewidth less than 0.5 meV show equal dephasing times in parallel and crossed configuration, whereas samples with larger linewidths (with exception of the 30-nm QW) exhibit remarkable differences in the two T_2 values which amount to a factor of almost 2 in some cases. The data show that the value of R is strongly sample dependent. Considering all data points, it reveals no simple correlation with the thickness of the QW but rather with the differing growth conditions of the various laboratories. This experimental finding provides evidence for attributing the change of T_2 with polarization configuration to an extrinsic rather than to an intrinsic property of the quantum-well samples. In the set of single quantum wells (triangular points in Fig. 5) contained within the same sample, and therefore likely to exhibit the same interfacial quality, we observe a clear well width dependence of the T_2 change. Since in narrower wells the exciton is more sensitive to interfacial quality, this observation may point to the role of interface disorder in mixing of the exciton transitions. By and large, our findings tend to support disorder-induced mixing of the excitonic levels as a potential mechanism for generating the apparent polarization dependence of T_2 values.

CONCLUSIONS

In conclusion, we have developed a model to explain a number of time-resolved and time-integrated self-diffraction DFWM measurements in terms of coupling of either the initial or final states of the σ^+ and σ^- exciton transitions in quantum wells. This simple model allows an interpretation of the different dephasing times observed for the parallel and perpendicular polarization configurations. The decay of the signal for parallel polarization is the true T_2 time. The perpendicular decay constant gives some measurement of the inhomogeneity of the disorder coupling. The model also consistently explains the apparent transformation from photon-echo to free-induction-decay behavior measured in Ref. 3 as the polarization configuration is changed. Again, the perpendicular behavior is not a true free induction decay but instead also measures the inhomogeneity of the disorder coupling.

The present model may also be supported by recent experiments in photon-echo configuration under an external magnetic field in quantum wells.[8] Without magnetic field and for perpendicular excitation of the hh exciton a faster decay was observed as compared to the parallel situation. With finite magnetic field Zeeman splitting produced beats and the decay of the parallel and perpendicular excitations became comparable. We explain this behavior as follows. The Zeeman splitting will reduce the effective coupling due to the disorder since it brings the degenerate levels (without disorder) out of resonance. Then the Zeeman splitting becomes relevant and the different dephasing behavior is reduced.

Work is currently under way to obtain a clearer microscopic picture of the disorder-induced coupling.

ACKNOWLEDGMENTS

We are indebted to K. Ploog, MPI für Festkörperforschung, Stuttgart, R. Hey, Paul Drude Institut, Berlin, K. Köhler, Fraunhofer Institut für Angewandte Festkörperphysik, Freiburg, and Y. Horikoshi, NTT Basic Research Laboratories, S. Musashino-shi/Japan for the supply of their samples. Stimulating and fruitful discussions with J. Shah, S. Cundiff, S. Schmitt-Rink, S. W. Koch, E. O. Göbel, and J. Feldmann are gratefully acknowledged. This work has been supported in part (D.B.) by the Deutsche Forschungsgemeinschaft.

*Present address: Shell Research Limited, Thornton Research Centre, P.O. Box 1, Chester CB1 3SH, U.K.

[1]I. D. Abella, N. A. Kurnit, and S. R. Hartmann, Phys. Rev. **141**, 391 (1966).

[2]S. Schmitt-Rink, D. Bennhardt, V. Heuckeroth, P. Thomas, P. Haring, G. Maidorn, H. Bakker, K. Leo, D.-S. Kim, J. Shah, and K. Köhler, Phys. Rev. B **46**, 10 460 (1992).

[3]S. T. Cundiff, H. Wang, and D. G. Steel, Phys. Rev. B **46**, 7248 (1992).

[4]G. Bastard, *Wave Mechanics Applied to Semiconductor Heterostructures* (Les Editions de Physique, Les Ulis, France, 1988).

[5]A. Honold, T. Saku, Y. Horikoshi, and K. Köhler, Phys. Rev. B **45**, 6010 (1992).

[6]K. Leo, J. Shah, S. Schmitt-Rink, and K. Köhler, in *Proceedings of the 7th International Symposium on Ultrafast Processes in Spectroscopy, Bayreuth, Germany,* edited by A. Laubereau

and A. Seilmeier, IOP Conf. Proc. No. 126 (Institute of Physics, Bristol, 1992), p. 411.
[7]H. H. Yaffe, Y. Prior, J. P. Harbison, and L. T. Florez, in *Proceedings of the 2nd Conference on Quantum Electronics Laser Science, 1991,* Technical Digest Series No. 11 (Optical Society of America, Washington, D.C., 1991), p. 196.
[8]O. Carmel and I. Bar-Joseph, Phys. Rev. B **47**, 7606 (1993).
[9]M. Wegener, D. S. Chemla, S. Schmitt-Rink, and W. Schäfer, Phys. Rev. A **42**, 5675 (1990).
[10]S. Bar-Ad and I. Bar-Joseph, Phys. Rev. Lett. **66**, 2491 (1991).